Effect of substrate bias voltage on hybridization and tribomechanical properties of ultrathin amorphous carbon films deposited by radio-frequency sputtering

J. Xie and K. Komvopoulos*

Department of Mechanical Engineering, University of California, Berkeley, CA 94720, USA

Abstract

Ultrathin amorphous carbon (*a*-C) films were deposited on Si(100) substrates under low-pressure, radio-frequency sputtering conditions of varying substrate bias voltage in pure Ar atmosphere. The surface roughness and tribomechanical properties of the *a*-C films were measured with an atomic force microscope and a surface force microscope, respectively. Insight into tetrahedral (sp^3) and trigonal (sp^2) atomic carbon hybridization was obtained from the deconvoluted C1s core level peak of X-ray photoelectron spectroscopy spectra. Energetic particle collision theory was used to correlate hybridization and tribomechanical properties to low-pressure plasma discharge conditions. The results are interpreted in the context of Ar^+ ion collisions with carbon atoms at the growing film surface, followed by collision cascades between excited carbon atoms and other surface carbon atoms, resulting either in the removal of weakly-bonded carbon atoms and the dominance of sp^3 hybridization or the development of thermal spikes leading to sp^2 hybridization. Particle collision analysis shows that the sp^3 fraction is a function of the Ar^+ ion flux, sputtering yield of target carbon atoms, and kinetic energy of surface carbon atoms, in good qualitative agreement with experimental results of the sp^3 fraction versus substrate bias voltage.

---

*Corresponding author:
K. Komvopoulos: Tel.: 510-642-2563, Fax: 510-642-5539, E-mail: kyriakos@me.berkeley.edu

Submitted to the *Journal of Applied Physics* on June 3, 2014.

1. Introduction

Amorphous carbon (*a*-C) films have been at the frontline of thin-film research for a long time mainly because of the excellent physical properties, chemical inertness, transparency, and potential as protective overcoats of these films in several leading technologies, such as hard-disk drives and microelectromechanical devices.[1–3] Among various carbon film deposition methods,[4] mass-selected ion-beam deposition,[5] filtered cathodic vacuum arc,[6] and laser ablation[7] use energetic carbon ions as film-forming precursors. Tetrahedral (sp^3) carbon atom hybridization due to energetic carbon ions leads to the formation of a three-layer film structure consisting of an interface layer, the bulk film, and a surface layer,[8] which can be explained by the subplantation model.[3]

Conversely to deposition methods using ionized film-forming precursors, radio frequency (rf) sputtering, one of the most common film deposition techniques, uses low-energy neutral carbon atoms or clusters of atoms to form *a*-C films. Sputtering is an advantageous thin-film deposition process because of its intrinsic low levels of input energy, temperature, and vacuum compared to deposition methods using energetic ions as film-forming precursors. Inert ion bombardment of the growing film surface during sputtering enables tailoring of the film properties without altering the chemical environment of the film. By controlling the absorbed rf power, substrate bias voltage, deposition time, working pressure, and flow rate of process gas, ultrathin *a*-C films with sp^3 contents higher than 50 at% and nanohardness of ~39 GPa can be synthesized under optimum rf sputtering conditions.[9] The substrate bias voltage is a key deposition parameter because it directly affects the ion bombardment energy. While the hardness of *a*-C film increases with the bias voltage, above a critical substrate bias voltage (about –150 V) the film hardness decreases due to relaxation due to thermal spikes produced from intense ion bombardment.[9] The very low roughness of *a*-C films deposited under rf sputtering conditions of –200 V substrate bias voltage has been attributed to the enhancement of carbon atom diffusion at the film surface, whereas film roughening for substrate bias voltage above –200 V has been associated with re-sputtering and irradiation damage by the highly energetic Ar^+ ions.[10]

Although the effect of plasma discharge conditions (in particular, the substrate bias voltage) on

the growth and properties of sputtered *a*-C films has been investigated in previous studies, knowledge of the hybridization mechanisms and film structure-property interdependencies is sparse. Although insight into sp^3 hybridization under different substrate bias conditions has been provided by a previous probabilistic analysis of carbon atom hybridization in rf sputtered *a*-C films,[11] the effects of irradiation damage and thermal spikes were not considered and the substrate bias voltage was not varied above –200 V. Therefore, an in-depth study of the underlying hybridization mechanisms in the presence of thermal spikes on the structure of sputtered *a*-C films is timely and of high importance not only to the properties but also the stability of such ultrathin films.

The objective of this study is to elucidate the effects of plasma discharge conditions generated under different substrate bias voltages on the surface roughness, structure, and tribomechanical properties of ultrathin *a*-C films deposited by rf sputtering. The interdependence of surface topography (roughness), structure (hybridization), hardness, reduced elastic modulus, and coefficient of friction of sputtered *a*-C films on plasma discharge conditions is discussed in the light of atomic force microscope (AFM), surface force microscope (SFM), and X-ray photoelectron spectroscopy (XPS) measurements and results derived from particle collision analysis.

2. Experimental methods

2.1. Film deposition

Ultrathin *a*-C films were deposited on Si(100) substrates by sputtering a pure (~99.99%) graphite target with Ar^+ ions in a low-pressure sputtering system (Perkin-Elmer, Randex-2400 model). The vacuum chamber was first pumped down to a low base pressure (~2×10^6 Torr) to remove any residual gases adsorbed onto the chamber walls. The graphite target was then sputtered for 5–20 min, depending on the time of its exposure to the atmosphere, whereas the Si(100) substrate was sputtered for 3 min to remove an ~45-nm-thick surface layer, under conditions of working pressure p = 3 mTorr, forward rf power P_f = 250 W, and Ar gas flow rate f = 20 sccm. Film deposition was subsequently performed under plasma discharge conditions of adsorbed rf power P_a = 745–750 W, substrate bias voltage V_s between 0

and –300 V, and all other process parameters fixed, i.e., p = 3 mTorr, f = 20 sccm, and deposition time t = 0.4 min. a-C films deposited under these plasma discharge conditions have been found to demonstrate optimum properties.[9,12]

2.2. Atomic force microscopy

The film surface roughness was measured from 2 × 2 μm^2 images acquired with an AFM (NanoScope Ⅱ, Digital Instruments), which was operated in tapping mode. All AFM images were obtained with silicon tips of nominal radius of curvature equal to ~10 nm. The root-mean-square (rms) surface roughness of the a-C films was calculated as the mean value of at least four measurements obtained from different AFM images of each film surface.

2.3. Tribomechanical testing

The tribomechanical properties of the a-C films (i.e., nanohardness, reduced elastic modulus, and coefficient of friction) were studied with an SFM consisting of a special force transducer (Triboscope, Hysitron) interfaced with an AFM (NanoScope Ⅱ, Digital Instruments). The film mechanical properties were measured with a pyramidal diamond tip with a nominal radius of curvature equal to ~40 nm and tip shape function obtained by indenting a standard sample of ultra-smooth fused quartz of bulk hardness equal to 10 GPa. The indentation force was applied in an incremental fashion, using an isosceles triangular force profile of 20 μN peak force and loading/unloading times fixed at 6 s. The hardness and reduced elastic modulus of the a-C films were determined from the indentation force versus depth response, as detailed elsewhere.[9–12] At least five indentations were performed at different locations of each film surface.

Tribological tests were carried out with a conical diamond tip of nominal radius of curvature equal to 1 μm. In these tests, the normal force was varied in the range of 40–160 μN, whereas the sliding speed and the lateral displacement were fixed at 0.4 μm/s and 4 μm, respectively. The coefficient of friction (defined as the ratio of the measured friction force to the applied normal force) was calculated as the average of 300 coefficient of friction measurements obtained along the sliding track.

2.4. X-ray photoelectron spectroscopy

XPS spectra were acquired with a PHI model 5400 ESCA/XPS system. All of the XPS studies were performed under a vacuum pressure of <5 × 10^{-9} Torr using an Al-Kα anode X-ray source of 1486.6 eV energy, 0.1 eV energy step, and 0.025 eV analyzer energy resolution. After performing background noise subtraction with the Shirley method,[13] the C1s core level XPS spectra of the a-C films were fitted with 90% Gaussian–10% Lorentzian (GL) distributions and the sp^3 and sp^2 hybridization contents were calculated with a standard least–squares algorithm. Each GL distribution was associated with a certain chemical state of a characteristic binding energy. Atomic percentages of each constituent were calculated as the areas under corresponding GL distributions. To preserve the original surface chemical characteristics, the samples were not cleaned by Ar^+ ion bombardment before the XPS analysis.

3. Results and discussion

It has been previously shown[10] that the film thickness h mainly depends on the sputtering rate β of the target material (which is equal to the sputtering yield γ multiplied by the Ar^+ ion flux J_{Ar^+}) and the deposition time, i.e., $h \propto \beta t$. As shown later, the sputtering rate can be fixed by controlling the rf power and substrate bias voltage. Under these conditions, the film thickness is almost linearly proportional to the deposition time, and the thickness of ultrathin films can be determined by linear extrapolation of thickness data corresponding to relatively thicker films (i.e., t > 3 min with all other plasma discharge conditions fixed). Using this approach, the thickness of a-C films deposited under plasma discharge conditions of P_a= 745–750 W, V_s = –200 V, and t = 0.4 min was found to be equal to 4.64 nm.

Figure 1(a) shows the film roughness as a function of substrate bias voltage. The decrease in film roughness with the variation of the substrate bias voltage between 0 and –200 V is attributed to intensification of the Ar^+ ion bombardment onto the growing film surface. The smoothest film corresponds to plasma discharge conditions of V_s = –200 V. The increase in film roughness due to the change in V_s beyond –200 V is a result of excessive sputtering and irradiation damage. The film nanohardness and reduced elastic modulus were obtained from indentation force versus displacement

responses for indentation depth fixed at ~2.8 nm. Figures 1(b) and 1(c) show that the highest hardness and reduced elastic modulus correspond to V_s = –200 V, suggesting that a-C films deposited under these plasma discharge conditions exhibit the highest sp^3 content. The enhancement of the film nanomechanical properties with the variation of V_s from 0 to –200 V may be related to the beneficial effect of Ar^+ ion bombardment, whereas the degradation of the film properties with the variation of V_s beyond –200 V is due to excessive irradiation damage induced by the highly energetic Ar^+ ions.

The indirect effect of substrate bias voltage on the mechanical properties of a-C films may be explained by considering the dependence of mechanical properties on the carbon-carbon bond strength of different hybridizations. The outermost s and p orbitals of carbon atoms form π and σ bonds in sp^2 hybridizations, but only σ bonds in sp^3 hybridizations. The stronger σ bonds in sp^3 hybridizations control the mechanical properties, whereas the π bonds are mainly responsible for the electrical and optical properties.[3] The elastic modulus E of the a-C films can be related to the mean coordination $\langle r \rangle$ of carbon-carbon bonds by $E = E_0(\langle r \rangle - 2.4)^{3/2}$, where $\langle r \rangle = (2n_2 + 3n_3 + 4n_4)/(n_2 + n_3 + n_4)$ and n_i is the number of atoms with i bonds.[14,15] For a-C films, n_2, n_3, and n_4 represent the number of carbon atoms in sp^1, sp^2, and sp^3 bonding configurations, respectively. Moreover, the film hardness H can be approximately related to the elastic modulus by $H \approx E/10$ (Ref. 16). The former relations of the film elastic modulus and hardness indicate an increase in stiffness and plastic flow resistance of the a-C films with increasing coordination, implying an improvement of the film mechanical properties with increasing sp^3 fraction.

Figure 2 shows the variation of the coefficient of friction of a-C films with the substrate bias voltage and normal force. The decrease of the coefficient of friction with increasing normal force for fixed V_s suggests predominantly elastic film deformation, under the present test conditions. This is because the coefficient of friction of elastically deformed surfaces is inversely proportional to the cubic root of the normal force and the friction force is mainly due to the effects of adhesion and surface roughness.[12] The lowest coefficient of friction corresponding to V_s = –100 V, regardless of applied normal

force, is attributed to film shear resistance and surface roughness effects on the friction characteristics. Considering that the main friction mechanisms of smooth sliding surfaces are adhesion and plowing, which depend on the shear resistance and hardness of the sliding surfaces, respectively, i.e., the *a*-C film in the present tests since the diamond tip is essentially rigid, the lowest coefficient of friction for V_s = –100 V represents a compromise in sp^3 hybridization in favor of sp^2 hybridization, resulting in moderately decreased film plastic shear resistance and hardness, which reduces the contributions of adhesion and plowing to the coefficient of friction.

Figure 3 shows the effect of substrate bias voltage on the C1s core level XPS spectrum of *a*-C films. The six GL peaks fitted to the spectra represent different types of carbon-carbon and carbon-oxygen bonding. GL distributions 1–3 correspond to sp^1-, sp^2-, and sp^3-coordinated carbon bonding, whereas GL distributions 4–6 correspond to different binding states of carbon atoms with oxygen atoms chemisorbed onto the film surface upon exposure to the ambient. The full width at half magnitude of GL distributions 1–3 and 4–6 is in the range of 1.4–1.6 eV and 2.85–2.95, respectively. The spectra demonstrate significant intensification of GL distribution 3 for V_s = –100 V, suggesting an increase in sp^3 fraction due to energetic Ar^+ ion bombardment. Because the tribomechanical properties of carbon are controlled by the strong σ bonds existing only in sp^3 carbon configurations,[3,9,16,17] it may be inferred that energetic ion bombardment enhanced sp^3 carbon hybridization and, in turn, the film mechanical and tribological properties.

Figure 4 shows the effect of substrate bias voltage (energetic Ar^+ ion bombardment) on the sp^2 and sp^3 fractions. The statistical data included in this figure were calculated from XPS spectra obtained from three different locations on each film surface. The sp^3 fraction increases whereas the sp^2 fraction decreases with the variation of V_s from 0 to –200 V; however, an opposite trend is observed with the variation of V_s from –200 to –300 V.

Table I gives statistical results of the rms roughness R_q, hardness H, reduced elastic modulus $E^* = E/(1-\nu^2)$, coefficient of friction μ, and sp^3 and sp^2 hybridization contents of *a*-C films for

V_s between 0 and –300 V. The lowest roughness (R_q = 0.1 nm) and best mechanical properties, i.e., highest hardness (H = 34.2 GPa), reduced elastic modulus (E^*= 190.5 GPa), and sp^3 content (~50 at%), correspond to V_s = –200 V (film C) and the lowest coefficient of friction ($\mu \approx 0.15$) to V_s = –100 V (film B). The smoothness and better mechanical properties of film C correlate with the high sp^3 content, which is attributed to the bombardment of energetic Ar^+ ions, whereas the low coefficient of friction of film B correlates with the increase of the sp^2 content.

The results shown in Figs. 3 and 4 and Table I can be explained in the context of thermodynamic principles governing carbon atom hybridization in rf sputtered a-C films and the significant effect of the Ar^+ ion bombardment intensity, which strongly depends on the potential difference between the substrate and bulk plasma.[18] Under film deposition conditions of relatively intense Ar^+ ion bombardment, the relatively weaker sp^2 configurations are preferentially removed from the three-dimensional a-C network, increasing the percentage of the stronger sp^3 configurations. However, above a critical ion kinetic energy, excessive irradiation damage (thermal spikes) induced by the highly energetic Ar^+ ions degrades the film quality. Thus for the plasma discharge conditions of this study (P_a = 745–750 W, p = 3 mTorr, f = 20 sccm, and t = 0.4 min), optimum film deposition conditions occurred for V_s = –200 V, leading to the formation of high-quality a-C films.

Thin-film deposition by sputtering comprises three main stages: (a) sputtering off of film-forming atoms from a high-purity target material by impinging energetic Ar^+ ions, (b) transport of sputtered off atoms or clusters of atoms through the plasma space, and (c) atom diffusion at the surface of the growing film, resulting in chemical bonding with existing surface atoms. Therefore, to interpret the dependence of the structure and tribomechanical properties of a-C films on the plasma discharge conditions, it is instructive to consider the characteristics of low-pressure rf discharges, particularly the significance of power, working pressure, substrate bias voltage, and substrate surface temperature in each of the aforementioned stages of the sputtering process.

Carbon atom flux onto the growing film surface depends on the flux of incident Ar^+ ions J_{Ar^+}

onto the target surface and the sputtering yield γ of target carbon atoms (defined as the number of carbon atoms ejected from the bombarded target surface per incident Ar^+ ion). For parallel-plate, capacitive, electropositive low-pressure Ar discharges, such as those in the present study, J_{Ar^+} is given by[10]

$$J_{Ar^+} = \frac{P_a}{eA[2V_p - (V_t + V_s)]} \tag{1}$$

where e is the electron charge, A is the electrode area (= 324 cm^2 for both the target and the substrate of the present system), and V_p, V_t, and V_s are time-average voltages of the plasma bulk, target, and substrate, respectively. For fixed working pressure, $V_p \approx 10$ eV and $V_t + V_s$ is almost constant (Table II); hence Eq. (1) yields that $J_{Ar^+} \propto P_a$.

It is known that the sputtering yield depends on the energy of impinging Ar^+ ions.[19] On the basis of the sputtering theory introduced by Sigmund,[20] Matsunami et al.[21] obtained sputtering yield estimates for various ion-target combinations and derived an empirical formula of ion-induced sputtering yield Y given by

$$Y = 0.42 \frac{\alpha^* Q\, K\, s_n(\varepsilon)}{U_s[1 + 0.35\, U_s\, s_e(\varepsilon)]} \left[1 - \left(\frac{E_{th}}{E_i}\right)^{1/2}\right]^{2.8} \tag{2}$$

where α^* and Q are empirical parameters, K is a conversion factor, s_n and s_e are the reduced nuclear and electronic stopping cross sections, respectively, ε is the reduced ion energy, U_s is the sublimation energy of the target material, and E_i is the kinetic energy of the incident Ar^+ ions (expressed in eV). For graphite, $Q = 3.1 \pm 0.9$ and $U_s = 7.37$ eV.[21,22] For dominant nuclear stopping, α^* and E_{th} are given by[21]

$$\alpha^* = 0.08 + 0.164 \left(\frac{M_2}{M_1}\right)^{0.4} + 0.0145 \left(\frac{M_2}{M_1}\right)^{1.29} \tag{3a}$$

$$\frac{E_{th}}{U_s} = 1.9 + 3.8 \left(\frac{M_2}{M_1}\right)^{-1} + 0.134 \left(\frac{M_2}{M_1}\right)^{1.24} \tag{3b}$$

whereas s_n, s_e, ε, and K are given by[23–25]

$$s_n = \frac{3.44\varepsilon^{1/2} \ln(\varepsilon + 2.718)}{1 + 6.355\varepsilon^{1/2} + \varepsilon(-1.708 + 6.882\varepsilon^{1/2})} \tag{3c}$$

$$s_e = 0.079 \left[\frac{(M_1 + M_2)^{3/2}}{M_1^{3/2} M_2^{1/2}}\right] \left[\frac{Z_1^{2/3} Z_2^{1/2}}{\left(Z_1^{2/3} + Z_2^{2/3}\right)^{3/4}}\right] \varepsilon^{1/2} \tag{3d}$$

$$\varepsilon = \left[\frac{0.03255}{Z_1 Z_2 \left(Z_1^{2/3} + Z_2^{2/3}\right)^{1/2}}\right]\left[\frac{M_2}{M_1 + M_2}\right] E_i \tag{3e}$$

$$K = 8.478\left[\frac{Z_1 Z_2}{\left(Z_1^{2/3} + Z_2^{2/3}\right)^{1/2}}\right]\left[\frac{M_1}{M_1 + M_2}\right] \tag{3f}$$

where M_1, Z_1 and M_2, Z_2 are the mass and atomic number of incident energetic Ar^+ ions and carbon atoms, respectively.

Equations (1)–(3) were used to calculate J_{Ar^+} and γ under the present plasma discharge conditions. Table II shows the effect of process parameters (i.e., P_a, V_b, and V_s) on J_{Ar^+} and γ. Although J_{Ar^+} is essentially insensitive to variations in V_b and V_s, γ decreases as V_b and V_s change from –1750 to –1400 V and 0 to –300 V, respectively.

Atom flux on the growing film surface depends on the sputtering rate of target atoms $\beta = \gamma J_{Ar^+}$ and the scattering intensity of film-forming atoms travelling through the plasma space, which is inversely proportional to λ/L, where L is the target-substrate distance and λ is the mean free path of travelling atoms, given by[19]

$$\lambda = \frac{k_B T}{\sqrt{2}\pi d^2 p} \tag{4}$$

where k_B is the Boltzmann constant, T is the bulk plasma temperature, which is much higher than room temperature,[26] and d is the atom diameter (<3 Å for carbon). For a target-substrate distance L = 7 cm (fixed in this study) and p = 3 mTorr, Eq. (4) yields λ > 10 cm. Thus carbon atom scattering in the Ar plasma was not an important factor during film deposition under the present plasma discharge conditions because λ/L > 1.

The kinetic energy E_C transferred to carbon atoms at the growing film surface by elastic collisions with impinging Ar^+ ions is given by[26]

$$E_C = \frac{4M_1M_2}{(M_1+M_2)^2} E_i \sin^2\left(\frac{\theta}{2}\right) \tag{5}$$

where θ is the ion incidence angle. Thus, substituting M_1 = 39.9 and M_2 = 12 in Eq. (5) and integrating, the average kinetic energy of surface carbon atoms $\bar{E}_{\mathrm{C}}$ is given by

$$\bar{E}_{\mathrm{C}} = 0.355\bar{E}_i \tag{6}$$

where $\bar{E}_i$ is the average kinetic energy of bombarding Ar^+ ions.

Excited carbon atoms may collide with other carbon atoms at the film surface. The probability of this event is proportional to the nuclear stopping cross section S_n given by[27]

$$S_n = \frac{C_m \bar{E}_C^{(1-2m)}}{1-m}\left[\frac{4M_1M_2}{(M_1+M_2)^2}\right]^{(1-m)} \tag{7}$$

where C_m is a constant that depends on m, which can be obtained from the Thomas-Fermi screen function for different ranges of reduced ion energy ε (Ref. 28). At the surface of a sputtered *a*-C film, $\varepsilon < 0.2$ and $m = 1/3$ (Ref. 11); hence $S_n = \xi \bar{E}_C^{1/3}$, where $\xi = 6.05 \times 10^{-19}$ m^2.

The energy of surface carbon atoms excited by impinging Ar^+ ions may be dissipated by collisions with other surface carbon atoms, resulting in the removal of weakly bonded carbon atoms and, consequently, the formation of *a*-C films with high sp^3 content. The number of collisions of an excited carbon atom with other surface carbon atoms is given by $N = J_C/J_{\mathrm{Ar}^+} = \gamma J_{\mathrm{Ar}^+}/J_{\mathrm{Ar}^+} = \gamma$, where J_C is the carbon atom flux. The energy of excited carbon atoms may also be dissipated in the form of thermal spikes, a process resulting in thermal relaxation which is conducive to sp^2 hybridization. The number of surface carbon atoms migrating from high- to low-density domains per incident carbon atom is approximately given by $\eta \approx 0.016(\bar{E}_{\mathrm{C}}/3.1)^{5/3}$ (Ref. 29). A carbon atom arriving at the growing film surface may bounce of the surface, sputter N weakly bonded surface carbon atoms, or generate thermal spikes causing the migration of η surface carbon atoms. The removal of weakly bonded carbon atoms increases the sp^3 fraction, whereas thermal spikes increase the sp^2 fraction. Under the assumption of equal probabilities for these two phenomena, it follows that $sp^3/(sp^2 + sp^3) \propto N/(N + \eta)$. Thus considering that sp^3 hybridization also depends on J_{Ar^+} and S_n, which control the total number of collisions between incident Ar^+ ions and surface carbon atoms and the probability of such a collision event, respectively, the sp^3 fraction can be expressed as

$$\frac{sp^3}{sp^2+sp^3} \propto J_{\mathrm{Ar}^+}\, S_n \frac{N}{N+\eta} \tag{8}$$

For low-pressure rf sputtering without magnetron, J_{Ar^+} depends on P_a; thus the Ar^+ ion flux on the growing film surface is almost the same with that on the target surface [Eq. (1)]. Substitution of $S_n = \xi \bar{E}_C^{1/3}$, $N = \gamma$, and $\eta \approx 0.016(\bar{E}_\mathrm{C}/3.1)^{5/3}$ into Eq. (8) gives

$$\frac{sp^3}{sp^2+sp^3} \propto \xi J_{\mathrm{Ar}^+}\, \bar{E}_\mathrm{C}^{\;1/3} \frac{\gamma}{\gamma+0.016(\frac{\bar{E}_\mathrm{C}}{3.1})^{5/3}} \tag{9}$$

The validity of Eq. (9) can be assessed by comparing the measured sp^3 content of a-C films deposited under plasma discharge conditions of different substrate bias voltage with analytical results obtained from Eq. (9). As shown in Fig. 5, the experimental and analytical predictions of the sp^3 fraction follow a similar trend. (Eq. (9) gives results is in units of eV/s because J_{Ar^+} and S_n are in units of atoms/m^2·s and eV·m^2, respectively.) For $V_s = 0$ (insignificant Ar^+ ion bombardment), the removal of weakly bonded carbon atoms at the growing film surface is negligible and Eq. (9) yields $sp^3/(sp^2 + sp^3) \propto \bar{E}_\mathrm{C}^{\;1/3}$, implying low sp^3 content with low $\bar{E}_\mathrm{C}$. Optimum plasma discharge conditions occur for $V_s =$ –200 V, because weakly bonded carbon atoms are effectively sputtered off by bombarding Ar^+ ions without damage to the film structure. The present analysis predicts a maximum sp^3 fraction for substrate bias voltage of –183 V, which is close to the experimentally predicted optimum bias voltage (–200 V).

4. Conclusions

The effect of substrate bias voltage on the tribomechanical properties and hybridization of rf sputtered ultrathin a-C films was examined both experimentally and analytically. Under plasma discharge conditions of substrate bias voltage equal to –200 V, a-C films demonstrate minimum surface roughness and maximum reduced elastic modulus, hardness, and sp^3 fraction, whereas films deposited under conditions of –100 V substrate bias voltage exhibit minimum coefficient of friction. These results reveal a strong substrate bias (energetic Ar^+ ion bombardment) effect on carbon atom hybridization. A particle collision analysis was used to explain the effect of ion bombardment on the sp^3 content of the rf sputtered a-C films. The analysis yields a proportionality relation of the sp^3 fraction in terms of the average kinetic energy of surface carbon atoms, Ar^+ ion flux, and sputtering yield, which shows a similar trend with the

variation of the experimentally measured sp^3 fraction with the substrate bias voltage and yields an estimate of optimum substrate bias voltage in close agreement with the experimental value. The results of this study confirm the dependence of the tribomechanical properties of *a*-C films on the sp^3 content and provide insight into competing effects, such as re-sputtering, irradiation damage, and thermal spikes caused by impinging energetic Ar^+ ions, on the structural integrity of rf sputtered *a*-C films.

Acknowledgments

This research was funded by the Computer Mechanics Laboratory, University of California, Berkeley. The XPS studies were carried out at the Molecular Foundry of the Lawrence Berkeley National Laboratory (Proposal No. 1502).

References

[1] Erdemir A and Donnet C 2006 *J. Phys. D: Appl. Phys.* **39** R311–27.

[2] Chu P K and Li L 2006 *Mater. Chem. Phys.* **96** 253–77.

[3] Robertson J 2002 *Mater. Sci. Eng. R* **37** 129–281.

[4] Lifshitz Y 1999 *Diamond Relat. Mater.* **8** 1659-76.

[5] Ishikawa J, Takeiri Y, Ogawa K and Takagi K 1987 *J. Appl. Phys.* **61** 2509–15.

[6] McKenzie D R, Muller D and Pailthorpe B A 1991 *Phys. Rev. Lett.* **67** 773–6.

[7] Kovarik P, Bourdon E B D and Prince R H 1993 *Phys. Rev. B.* **48** 12123–9.

[8] Davis C A, Amaratunga G A J and Knowles K M 1998 *Phys. Rev. Lett.* **80** 3280–3.

[9] Lu W and Komvopoulos K 1999 *J. Appl. Phys.* **86** 2268–77.

[10] Wan D and Komvopoulos K 2006 *J. Appl. Phys.* **100** 063307.

[11] Wan D and Komvopoulos K 2006 *Appl. Phys. Lett.* **88** 221908.

[12] Lu W and Komvopoulos K 2001 ASME *J. Tribol.* **123** 641–50.

[13] Shirley D A 1972 *Phys. Rev. B* **5** 4709–14.

[14] He H and Thorpe M F 1985 *Phys. Rev. Lett.* **54** 2107–10.

[15] Robertson J 1994 *Pure Appl. Chem.* **66** 1789–96.

[16] Robertson J 1992 *Phys. Rev. Lett.* **68** 220–3.

[17] Tsai H and Bogy D B *J. Vac. Sci. Technol. A* **5** 3287–312.

[18] Wan D and Komvopoulos K 2007 *J. Phys. Chem. C* **111** 9891–6.

[19] Ohring M 1992 *Materials Science of Thin Films – Deposition and Structure* (2nd edition, Academic, New York).

[20] Sigmund P 1969 *Phys. Rev.* **184** 383–416.

[21] Matsunami N, Yamamura Y, Itikawa Y, Itoh N, Kazumata Y, Miyagawa S, Morita K, Shimizu R and Tawara H 1984 *Atomic Data and Nuclear Data Tables* **31** 1–80.

[22] Yamamura Y, Matsunami N and Itoh N 1983 *Radiat. Eff. Defects Solids* **71** 65–86.

[23] Lindhard J, Nielsen V, Scharff M and Thomsen P V 1963 *Mat. Fys. Medd. Dan. Vid. Selsk.* **33**(No. 10) 1–42.

[24] Lindhard J, Scharff M and Schiøtt H E 1963 *Mat. Fys. Medd. Dan. Vid. Selsk.* **33**(No.14) 1–42.

[25] Lindhard J, Nielsen V and Scharff M 1968 *Mat. Fys. Medd. Dan. Vid. Selsk.* **36**(No. 10) 1–32.

[26] Lieberman M A and Lichtenberg A J 1994 *Principles of Plasma Discharges and Materials Processing* (Wiley, New York).

[27] Nastasi M and Mayer J W 2006 *Ion Implantation and Synthesis of Materials* (Springer-Verlag, Berlin Heidelberg, Germany) 49–61.

[28] Winterbon K B, Sigmund P and Sanders J B 1970 *Mat. Fys. Medd. K. Dan. Vidensk. Selsk.* **37**(No. 14) 1-73.

[29] Robertson J 1993 *Diamond Relat. Mater.* **2** 984–9.

TABLE I. Surface roughness, mechanical properties, coefficient of friction, and carbon atom hybridization of a-C films versus substrate bias voltage.

Film	V_s (V)	R_q (nm)	H (GPa)	E^* (GPa)	μ	sp^3 (at%)	sp^2 (at%)
A	0	0.160 ± 0.023	22.96 ± 4.70	163.38 ± 19.24	0.185 ± 0.010	9.2 ± 1.0	63.2 ± 1.9
B	–100	0.132 ± 0.012	25.45 ± 6.12	174.75 ± 32.86	0.153 ± 0.015	36.6 ± 4.6	38.4 ± 4.0
C	–200	0.100 ± 0.007	34.20 ± 9.17	190.50 ± 25.35	0.173 ± 0.021	49.9 ± 0.2	30.3 ± 2.3
D	–300	0.114 ± 0.002	19.78 ± 5.82	143.28 ± 17.62	0.182 ± 0.008	26.8 ± 6.5	49.0 ± 5.4

TABLE II. Effect of plasma discharge conditions on Ar^+ ion flux and sputtering yield.

Film	P_a (W)	V_t (V)	V_s (V)	J_{Ar^+} ($\times 10^{15}$ ions/cm^2 ·s)	γ
A	748	–1750	0	8.15	0.95
B	745	–1500	–100	8.87	0.90
C	750	–1450	–200	8.66	0.88
D	748	–1400	–300	8.39	0.80

List of Figures

Fig. 1 Effect of substrate bias voltage on (a) surface roughness, (b) nanohardness, and (c) reduced elastic modulus of a-C films deposited under plasma discharge conditions of P_f = 750 W, p = 3 mTorr, f = 20 sccm, and t = 0.4 min.

Fig. 2 Effect of substrate bias voltage on coefficient of friction of a-C films deposited under plasma discharge conditions of P_f = 750 W, p = 3 mTorr, f = 20 sccm, and t = 0.4 min for normal force equal to 40, 80, and 160 μN.

Fig. 3 C1s core level XPS spectra of a-C films deposited under plasma discharge conditions of (a) V_s = 0 and (b) V_s = –100 V and all other deposition parameters fixed (P_f = 750 W, p = 3 mTorr, f = 20 sccm, and t = 0.4 min). Each spectrum is fitted with six GL distributions corresponding to different types of carbon bonding.

Fig. 4 Effect of substrate bias voltage on sp^3 fraction of a-C films deposited under plasma discharge conditions of P_f = 750 W, p = 3 mTorr, f = 20 sccm, and t = 0.4 min.

Fig. 5 (a) Experimental and (b) analytical results showing the effect of substrate bias voltage on the sp^3 content of a-C films deposited under plasma discharge conditions of P_f = 750 W, p = 3 mTorr, f = 20 sccm, and t = 0.4 min.

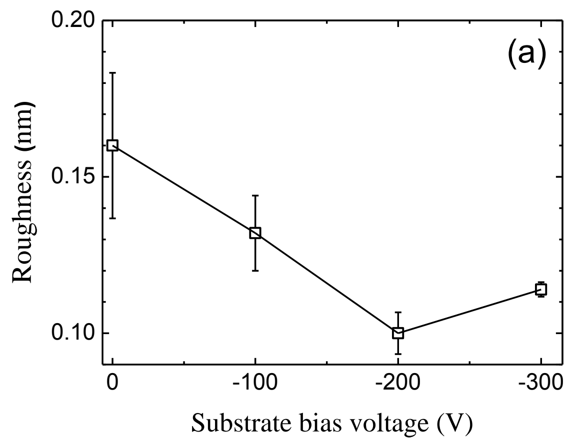

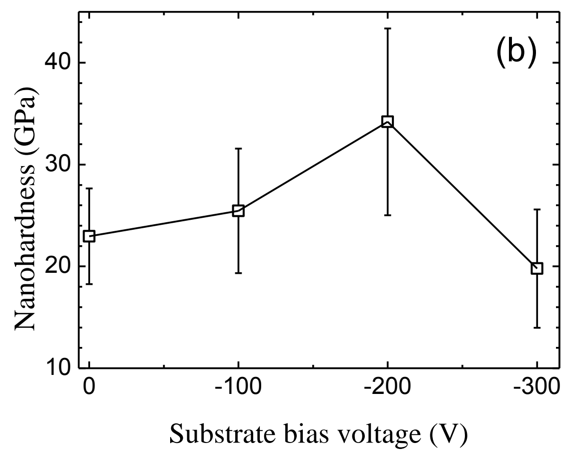

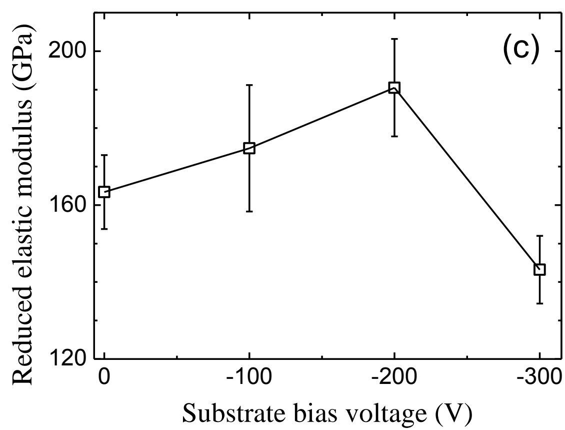

Figure 1

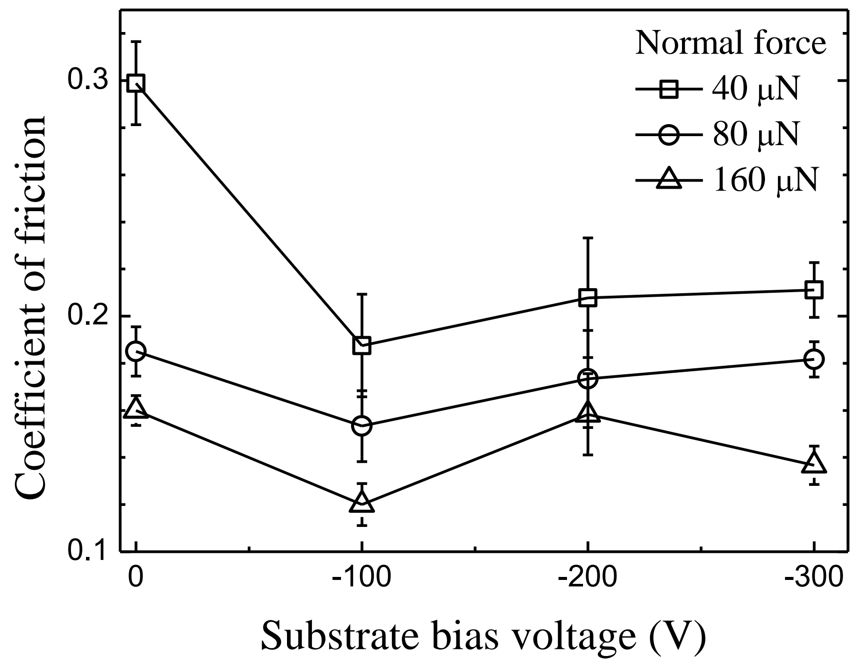

Figure 2

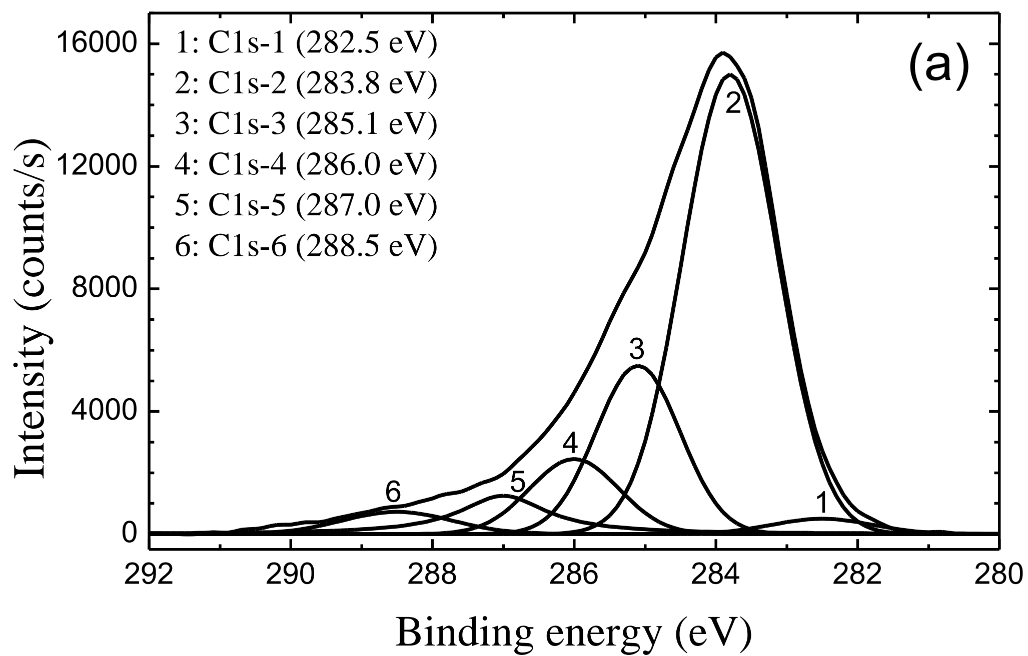

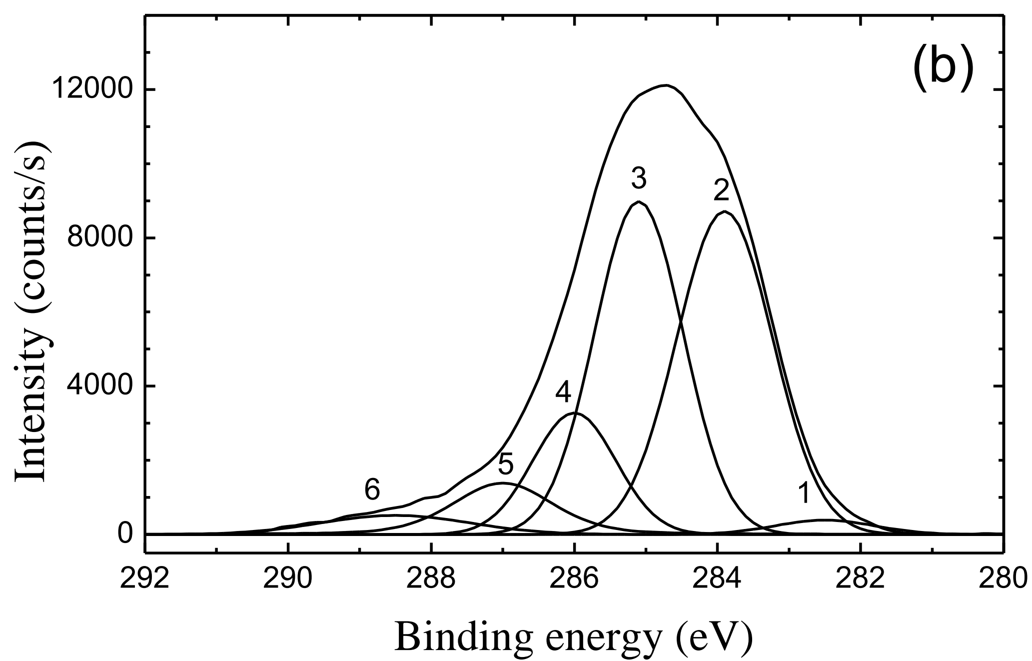

Figure 3

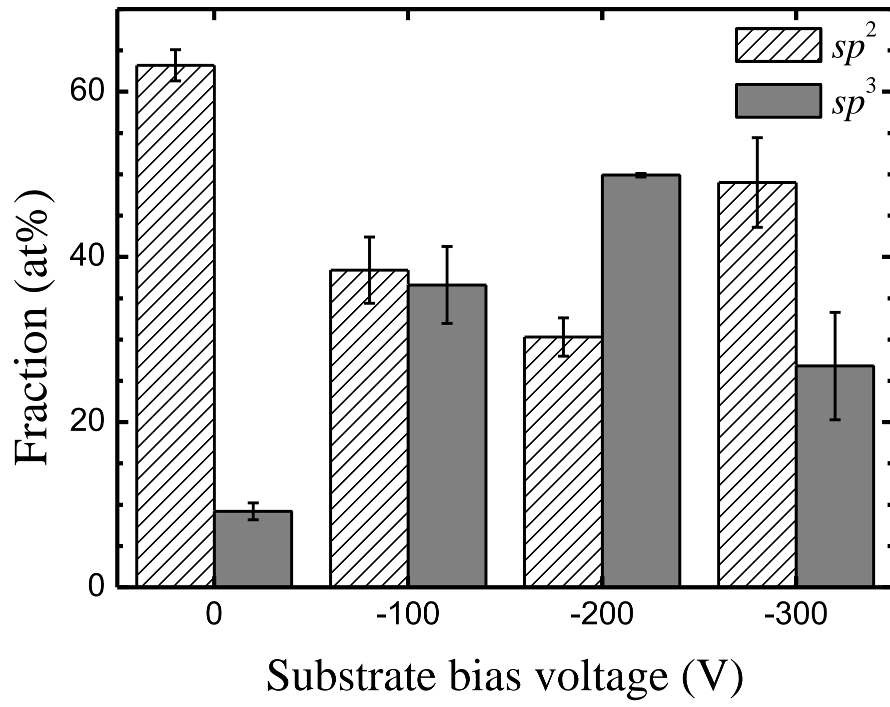

Figure 4

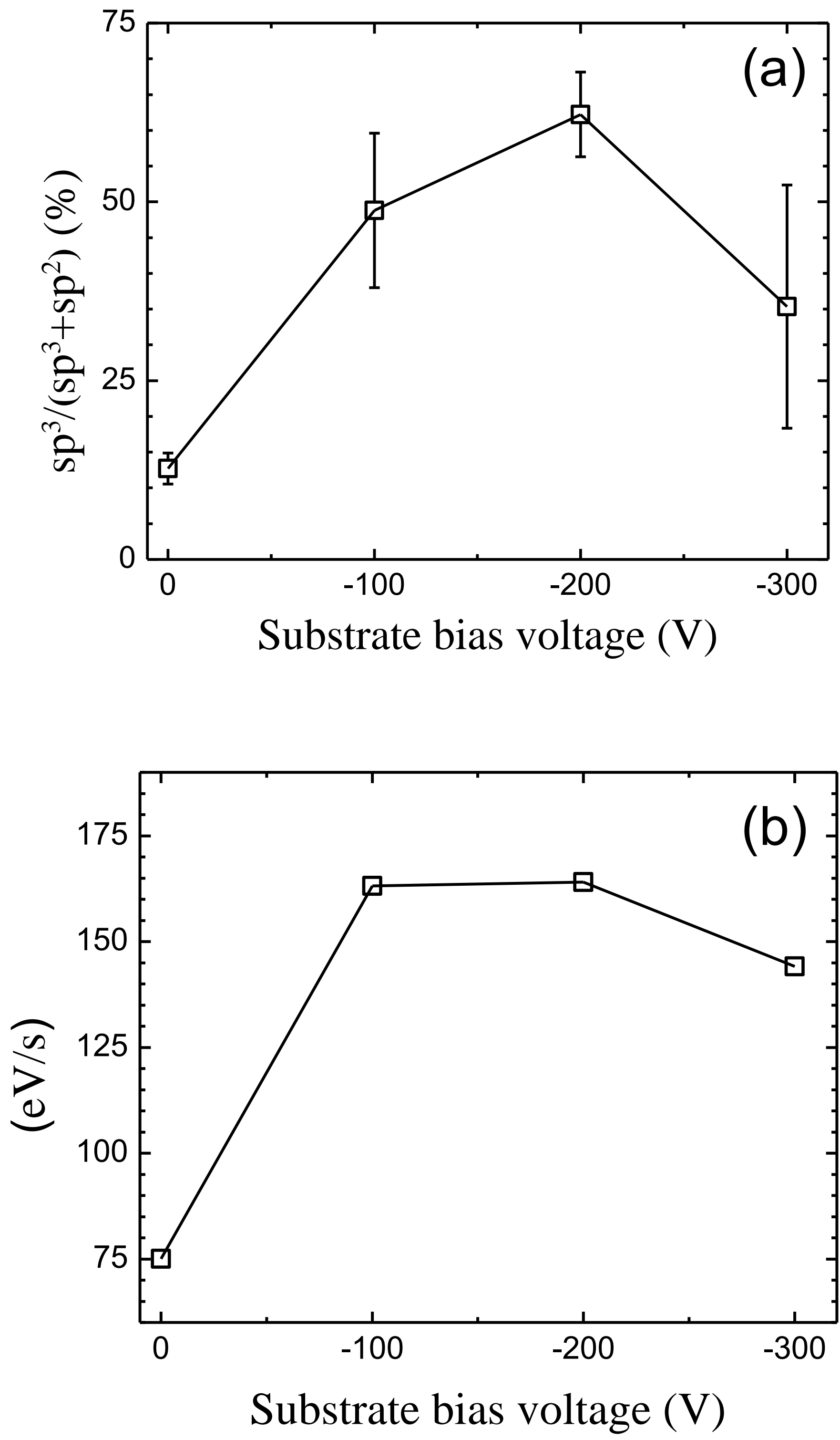

Figure 5